Summer Spatial Distribution of Copepods and Fish Larvae in Relation to Hydrography in the Northern Taiwan Strait

Chih-Hao Hsieh and Tai-Sheng Chiu*

Department of Zoology, National Taiwan University, Taipei, Taiwan 106, R.O.C.

Chih-Hao Hsieh and Tai-Sheng Chiu (2002) Summer spatial distribution of copepods and fish larvae in relation to hydrography in the northern Taiwan Strait. *Zoological Studies* **41**(1): 85-98. This study analyzed the spatial distribution of copepods and fish larvae in relation to hydrographic conditions in the northern Taiwan Strait during summer as the prevailing southwestern monsoon drives the surface warm water from the South China Sea into the Strait and causes subsurface water upwelling in the west. Cluster analysis based on copepod and fish larvae assemblages resulted in recognition of 4 groups, of which 3 major ones conformed to the hydrography. The western Taiwan Strait group was characterized by coastal and neritic species, the East China Sea group was dominated by oceanic species, and the eastern Taiwan Strait group consisted of both neritic and oceanic species. Analysis of dominant species also supports this result. Copepod abundance was positively related to water temperature and dissolved oxygen. The area of high copepod abundance did not correspond to the area of high primary productivity in the upwelling area, but occurred at a stable area downstream of the upwelling. Fish larva abundance was positively related to copepod abundance. http://www.sinica.edu.tw/zool/zoolstud/41.1/85.pdf

Key words: Species composition, Southwestern monsoon, South China Sea, East China Sea, Upwelling.

The Taiwan Strait, a shallow channel bounded by the southeastern China coast on the west and by Taiwan on the east, and connecting the East China Sea and South China Sea, serves as a pathway for migratory fishes between the 2 waters, and therefore it is an important fishing ground. The hydrographic conditions of the Strait are generally influenced by 3 current systems with seasonal variations, i.e., the Kuroshio, China coastal current, and South China Sea current, as well as river runoff from both mainland China and the island of Taiwan. When the southwestern monsoon prevails during summer, the Kuroshio branch does not enter the Strait, while warm water from the South China Sea penetrates through the Penghu Channel into the northern Taiwan Strait (Fang and Yu 1981, Fang 1982). Impeded by the Changyun Ridge, the surface and subsurface waters from the Penghu Channel flow in different directions. The light and warm surface water flows over the Ridge into the northeastern Taiwan Strait (hereafter the eastern Strait), while the heavy cold subsurface water is blocked by the Ridge and turns northwestward along local isobaths into the northwestern Taiwan Strait (hereafter the western Strait). Because of surface Ekman transport driven by the southwestern monsoon along the China coast, subsurface water originating from the Penghu Channel wells up and mixes with China coastal water in the western Strait (Xiao 1988, Jan et al. 1994). On the other side, surface water from the Channel flows into the eastern Strait and mixes with Taiwan coastal water. A detailed description of the summer hydrography of the Taiwan Strait was given by Jan et al. (1995). As oceanic physical processes influence the distribution of marine plankton (Boucher 1984, Boucher et al. 1987), variations in hydrographic conditions of the Taiwan Strait provide an opportunity to study the effects of physical processes on the spatial

---

* To whom correspondence and reprint requests should be addressed. Tel: 886-2-2363-0231 ext. 2128. Fax: 886-2-23634014.

distribution of copepods and fish larvae.

Although the Taiwan Strait is ecologically important for faunal exchange between the 2 marginal seas in the western Pacific, studies on the controlling factors of the distribution and abundance of fish larvae and zooplankton in the Strait are scarce. Tzeng and Wang (1992 1993) studied the seasonal dynamics of fish larvae and their relationship to the Tanshui River discharge. Chiu and Chang (1994) reported on the fish larvae fauna of the eastern Strait during winter and spring. Chiu and Chang (1995) studied diurnal cycling of fish larvae in the Tanshui River plume. Copepod species in the northern Taiwan Strait were reported by Tan (1967), Zheng et al. (1982) and Chen (1992), and in the Tanshui River estuary by Hsieh and Chiu (1998). Some information about the distribution and seasonal variation of phytoplankton, zooplankton, and fish larvae was also compiled (Zhu et al. 1988); however these studies were confined to the western Strait and did not discuss the influence of hydrographic patterns on these organisms.

Survivorship of fish larvae affects the recruitment success of fishes. Food availability is crucial for larval survival, especially at very early life stages when the yolk is exhausted. Copepods are the major component of marine zooplankton and thus are the main food source of fish larvae (Poulet and Williams 1991). It has been shown that salinity, temperature, and primary production have immense impacts on zooplankton distribution and abundance (Tremblay and Roff 1983, Thomas and Emery 1986, Fernandez et al. 1993). In this study, we examined the hydrographic influence on the trophic relationship between fish larvae and copepods, and tested the spatial overlap of copepods and fish larvae in the northern Taiwan Strait in summer. This work is a part of Taiwan Strait Marine Ecosystem project in compliance with the GLOBEC (Global Ocean Ecosystem Dynamic Program).

MATERIALS AND METHODS

Sampling

A cruise was carried out on 16-18 August 1999 on board the *Ocean Research II* with 11 stations (stations 5-15) in the northern Taiwan Strait and 4 stations (stations 1-4) in waters off northern Taiwan (Fig. 1). Fish larvae were collected using a round-mouthed ichthyoplankton net with a mouth diameter of 130 cm and mesh size of 1 mm, while zooplankton were collected using a standard North Pacific

zooplankton net with a mouth diameter of 45 cm and mesh size of 150 µm. A flowmeter was mounted at the center of the mouth of each net. The 2 nets were towed simultaneously and obliquely from near the bottom to the surface for surveying an average of total copepod and ichthyoplankton fauna. Ichthyoplankton samples were preserved with 95% alcohol, and zooplankton samples were preserved in seawater with 5% formalin. Vertical profiles of temperature, salinity, fluorescence and dissolved oxygen were obtained at each station from bottom to surface using a conductivity-temperature-depth (CTD) profiler (Sea-Bird Electronic) equipped with a fluorometer and an oxygen sensor. The fluorescence value was not calibrated but was used as an index of relative primary productivity. The current velocity was recorded using a shipboard ADCP (acoustic Doppler current profiler).

In the laboratory, each of the fish larvae in the ichthyoplankton samples was identified to species whenever possible. The number of individuals was then counted for each species. Fish larvae in zooplankton net samples were counted for estimating total abundance, but were not incorporated into cluster analysis in order to keep the data standardized. Abundance of fish larvae was expressed as the number of individuals per 1000 m^3. Copepods in zooplankton net samples were sub-sampled using a Folsom splitter until the sample size was reduced to 250-400 specimens.
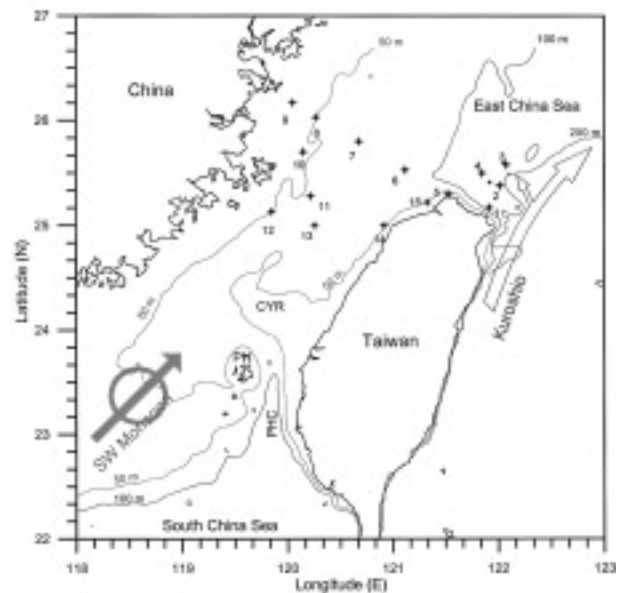

Fig. 1. Sampling stations for hydrographic data, fish larvae, and zooplankton in the northern Taiwan Strait, August 1999. (PH, Penghu Islands; PHC, Penghu Channel; CYR, Changyun Ridge).

Copepods were identified to species when possible, and the number of individuals of each species was recorded. Abundance of copepods was expressed as the number of individuals per m³.

Data analysis

Principal component analysis was used to characterize the hydrographic regions based on station data of bottom depth, surface water temperature, salinity, fluorescence, and dissolved oxygen (Pielou 1984). Cluster analysis was used to examine the association among sampling stations based on species percentage composition data (Pielou 1984). For copepods, only species which accounted for 2% or more of the total number of specimens in at least 1 station were included in the analysis. Species comprising less than 2% are considered rare species and might lead to derivation of erroneous relationships in the community analysis (Gauch 1983). Likewise for fish larvae, only species which accounted for 5% or more in at least 1 station were included. For normalizing the patchiness of zooplankton, data were square-root transformed (Krebs 1989). Normalized Euclidean distance was applied to measure the dissimilarity among stations, and Ward's method of grouping was used to obtain the correspondence dendrogram (Pielou 1984). Based on the abundance of dominant species of copepods (> 3%) and fish larvae (> 5%) of each region defined by principal

component analysis, canonical correspondence analysis was used to determine the relationship between dominant species and oceanographic conditions (Braak 1994). A generalized linear model (McCulliagh and Nelder 1983) was applied to examine the relationship between copepod abundance and the 5 oceanographic variables of bottom depth, surface water temperature, salinity, fluorescence, and dissolved oxygen; as well as the relationship between combined fish and copepod abundance and the 5 oceanographic variables. The best model was achieved by stepwise multiple regression analysis, and the variables were standardized before analysis. A *t*-test was used to examine the significance of the coefficients of the variables in the models and the α value set to 5%.

RESULTS

Hydrography

The depth-averaged current vectors in the northern Taiwan Strait during the survey period are plotted at flood and ebb stages respectively (Fig. 2). The water moves northeastward from the Strait to the East China Sea at ebb, and southwestward from the East China Sea to the Strait at flood tides. The surface water temperature and salinity contour plots of the northern Taiwan Strait indicate that the water is divided along the middle
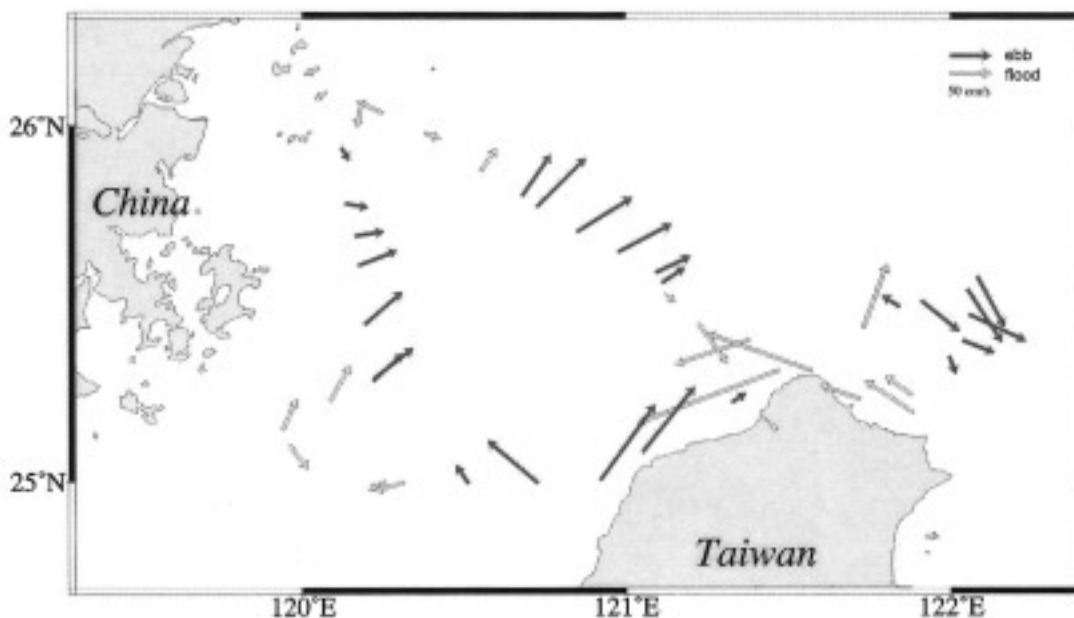

Fig. 2. Scatter plot of current vectors showing the depth-averaged current velocities at flood and ebb tides, respectively.

into 2 parts, with a relatively low salinity and high temperature in the eastern Strait, and a relatively high salinity and low temperature in the western Strait, except that an extremely low salinity was found off the Chinese coast (Fig. 3a, b). Evidence
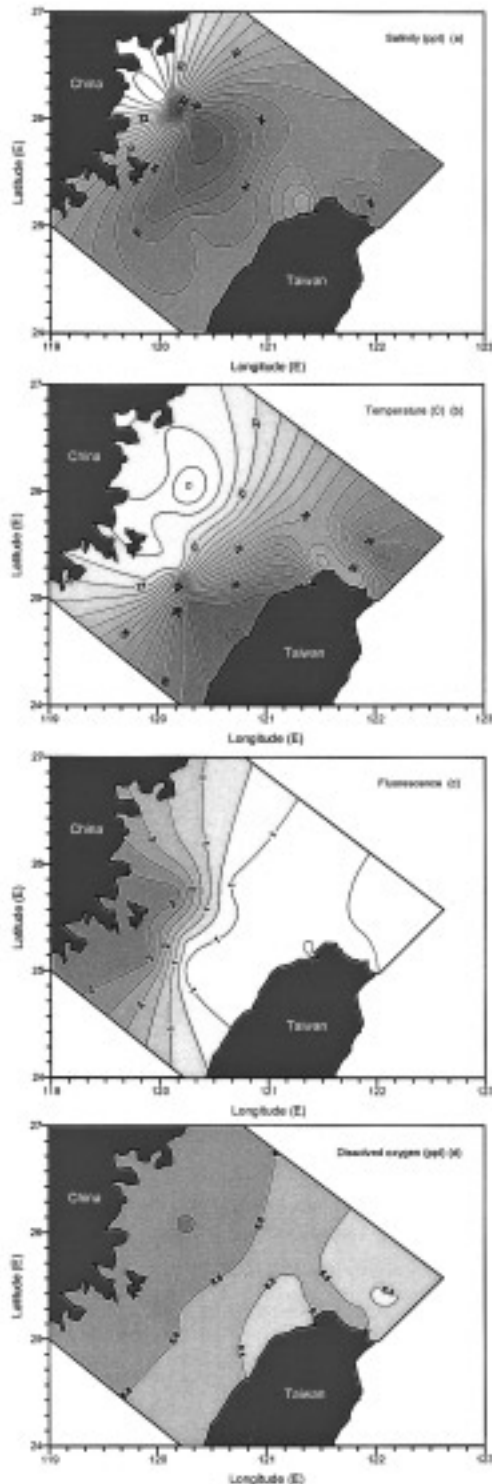

Fig. 3. Contour plots of surface salinity (a), temperature (b), fluorescence (c), and dissolved oxygen (d) in the northern Taiwan Strait.

of river runoff was obvious near shore (around stations 9 and 14-15) where 2 lenses of low salinity were found. The low temperature and high salinity of the western Strait reveals the occurrence of upwelling. During this study, the upwelling area was widespread (stations 7-8 and 10-13), indicating that the southwestern monsoon was driving water from the South China Sea along the coast of mainland China, forming an Ekman transport phenomenon. Surface water fluorescence and dissolved oxygen contour plots show that higher values were found in the western than that in the eastern Strait (Fig. 3c, d). According to the principal component analysis based on the 5 hydrographic variables, 15 stations were categorized into 3 regions: western Taiwan Strait - stations 7, 8, and 10-13; eastern Taiwan Strait - stations 5, 6, 14, and 15; and East China Sea - stations 1-4 (Fig. 4). The names are given according to the geographic regions where the stations are located. Station 9 is distinct from other stations because of its extremely low salinity as shown in figure 3a. For simplicity, station 9 is assigned to the western Taiwan Strait region due to its locality. The eigenvalues and component loadings of principal component analysis indicated that variables of bottom depth and temperature contrasted with those of fluorescence and dissolved oxygen, while salinity was less distinctive (Table 1).
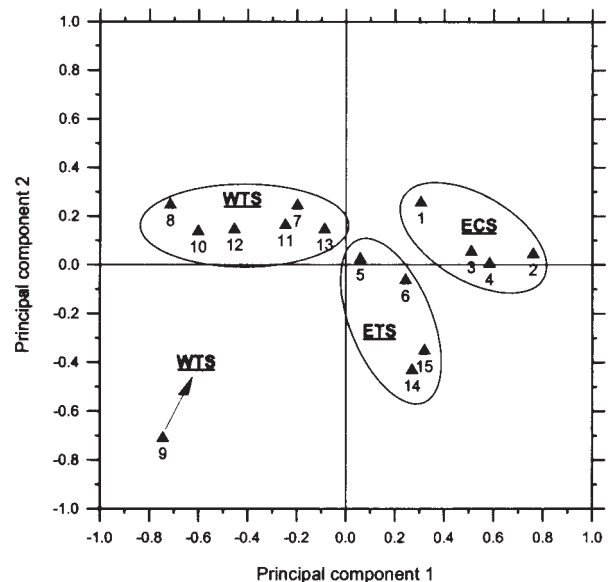

Fig. 4. Principal component analysis biplot based on bottom depth, surface water temperature, salinity, fluorescence, and dissolved oxygen, of 15 sampling stations indicating 3 hydrographic regions (WTS, western Taiwan Strait; ETS, eastern Taiwan Strait; ECS, East China Sea).

Species composition and distribution

In this study, 122 copepod species in 26 families were identified, with 116 to species and 6 to genus level (Table 2), and a total of 96 fish species in 46 families were identified, with 76 to species, 9 to genus, and 11 only to family (Table 3). Cluster analysis of stations based on the copepod composition shows 4 groups A1-A4 (Fig. 5a). The clusters of A1 (stations 8-12), A2 (stations 5 and 15), and A4 (1-4, 6, and 14) represent the western Strait, the eastern Strait, and the East China Sea groups respectively, but an extra cluster of A3 (7 and 13) was formed by interim stations. The clusters show 73.3% of stations matching the hydrographic regions; only stations 6, 7, 13, and 14 are contradictary to the hydrographic categories (Fig. 4). The dendrogram derived from the species composition of fish larvae also shows a fairly similar result (Fig. 5b), with B1 (stations 7-11), B3 (stations 4-6 and 14), and B4 (stations 1-3) representing the western Strait, the eastern Strait, and the East China Sea groups respectively. The fish larvae dendrogram also shows 73.3% stations matching the hydrographic regions with 4 stations (4, 12, 13 and 15) differing from the hydrographic categories. However, the dendrograms of copepods and fish larvae show 46.7% of similarity to each other, while stations 4-7 and 12-15 are categorized differently (Fig. 5).

Species compositions of copepods and fish larvae of the 3 hydrographic regions are listed in tables 2 and 3, respectively, and dominant species are highlighted in boldface. A canonical correspondence ordination biplot of dominant species of copepods and fish larvae shows the relationships between the species and oceanographic variables (Fig. 6). Of copepods, the dominant species can be separated into 3 groups. Group A, located in western Taiwan Strait with high fluorescence and dissolved oxygen contrasting with low temperature, salinity, and depth, is composed of *Acartia pacifica*, *Corycaeus lubbocki*, *Euterpina acutifrons*, and *Oithona brevicornis*. However, among the rest of the species, *Clausocalanus forcatus*, *Oithona plumifera*, and *Oncaea conifera* were located in deeper waters, preferred high temperature and salinity, and are assigned to group C. The species group of *Acrocalanus gibber*, *Canthocalanus pauper*, *Corycaeus dahli*, *Oithona attenuata*, *Oncaea venusta*, *Paracalanus pavus*, *Paracalanus serrulus*, *Parvocalanus crassirostris*, and *Temora turbinata*, located at a hydrographic intermediate, was assigned to group B (Fig. 6a). The first 2 canonical axes explain 36.5% of the hydrographic variance among copepod species groups. Among dominant fish larvae, species group A, composed of *Priacanthus macracanthus* and *Diaphus pacificus*, prefers high temperature at deeper water where fluorescence and dissolved oxygen are low. However, species group C, composed of *Leiognathus rivulatus*, *Nibea* sp., *Pseudosciaena* sp., and *Saurida elongata*, prefers high fluorescence and dissolved oxygen with low temperature at shallower depth. The remaining species forming group B, including *Apogon endekataenia*, *Auxis rochei*, *Ceratoscopelus warmingi*, *Diaphus theta*, *Encrasicholina heteroloba*, and *Trichiurus lepturus*, are associated with intermediate hydrographic factors (Fig. 6b). The first 2 canonical axes explain 38.19% of the hydrographic variance among fish larvae groups, and it is worth noting that both axes are feeble due to salinity variations.

Density of copepods and larval fish

Area contour plots of copepod and fish larvae abundances are shown in figure 7. Lenses of rela-

Table 1. Eigenvalues and component loadings of the principal components based on correlation of hydrographic factors

Principal component	1	2	3	4	5
Eigenvalue	3.254	1.095	0.369	0.282	0
Percentage	65.087	21.894	7.387	5.63	0.001
Cum. percentage	65.087	86.981	94.368	99.999	100
Loading					
Depth	0.446	0.288	0.828	0.18	-0.002
Temperature	0.529	-0.185	-0.13	-0.408	0.709
Salinity	-0.037	0.935	-0.258	-0.218	0.099
Fluorescence	-0.484	-0.069	0.448	-0.749	-0.006
Dissolved oxygen	-0.535	0.056	0.175	0.44	0.698

tive high densities of copepods and fish larvae are located in the northwest and southeast of the study area. However, higher fluorescence indices were located in the western Strait in agreement with the upwelling region, and with an area of higher dissolved oxygen as well (Fig. 3c, d). Apparently, higher abundances of copepods and fish larvae were located in vicinities of the upwelling region. Multiple regression analysis indicates that copepod abundance (C) was positively related to water temperature (T) and dissolved oxygen (D), but negatively related to fluorescence (FL) (C = 1.05 T + 1.65 DO - 0.55 FL, R^2 = 0.717, p = 0.0024, df = 11), and fish larvae abundances (F) were positively related to copepod abundance (F = 0.52, r = 0.521, p = 0.0463, df = 13).

DISCUSSSION

In this study, we found that the current velocity is higher in the eastern than in the western Taiwan Strait (Fig. 2; Jan et al. 1995). The water movement is primarily affected by western Pacific tides and causes the water from the East China Sea to mix with water in the Strait, especially on the eastern side. However, the mean flow in the Strait is generally northward during summer (Jan et al. 1995). Therefore, the diurnal tidal movement and the prevailing northward current may be the 2 forces that drive variations of copepod and larval fish fauna in the northern Strait.

The distribution of copepods and fish larvae was found to be linked to the hydrography in the northern Taiwan Strait during our examination of assemblages. Both copepod and fish larvae clusters showed 73.3% matching hydrographic categories (Fig. 6). However, only as low as 46.7% of similarity was found corresponding to copepod and fish larvae assemblages. In further analysis, we found that station groups of 1-3 and 8-10 were never mis-classified in the 3 comparisons -- hydrography vs. copepod, hydrography vs. fish larvae, and copepod vs. fish larvae, owing to their attributes of purity having been located at 2 ends of examined area. We may therefore define the

Table 2. Relative abundance (%) of copepods collected from the northern Taiwan Strait and southern East China Sea. Assemblages were categorized according to hydrographic regions. Dominant species of each region are marked in boldface

Family	Species	Assemblage categories		
		West Strait	East Strait	East China Sea
Order: Calanoida				
Acartiidae	*Acartia negligence*	0.04	1.53	1.57
	Acartia longiremis	0.00	0.00	0.00
	Acartia omori	0.00	0.00	0.06
	Acartia pacifica	3.30	0.46	0.06
	Acartia sp.	0.00	0.18	0.00
Arietellidae	*Metacalanus aurivillii*	0.05	0.00	0.00
Calanidae	*Calanoides carinatus*	0.04	0.00	0.00
	Calanus sinicus	0.00	0.17	0.13
	Canthocalanus pauper	4.16	6.24	6.25
	Cosmocalanus darwinii	0.00	0.18	0.23
	Mesocalanus tenuicornis	0.00	0.00	0.08
	Nannocalanus minor	0.18	0.40	0.00
	Neocalanus gracilis	0.04	0.24	0.19
	Undinula vulgaris	0.58	1.41	1.97
Cadaciidae	*Candacia bipinnata*	0.00	0.00	0.07
	Candacia catula	0.00	0.09	0.00
	Candacia discaudata	0.14	0.00	0.00
	Candacia elongata	0.05	0.00	0.00
	Candacia copepodid	0.37	0.40	0.80
	Paracandacia truncata	0.03	0.00	0.00
Centropagidae	*Centropages orsinii*	0.22	0.55	0.07
	Centropages furcatus	0.04	0.00	0.26

Table 2. (Cont.)

Family	Species	Assemblage categories		
		West Strait	East Strait	East China Sea
	Centropages gracilis	0.00	0.07	0.00
Clausocalanidae	*Clausocalanus arcuicornis*	0.04	0.07	0.07
	Clausocalanus brevipes	0.05	0.00	0.00
	Clausocalanus forcatus	0.80	1.88	4.04
	Clausocalanus ingens	0.00	0.00	0.19
	Clausocalanus minor	1.21	0.08	1.22
	Clausocalanus mastigophorus	0.09	0.09	0.26
	Clausocalanus parapergens	0.04	0.00	0.00
	Clausocalanus pergens	0.16	0.00	0.00
	Ctenocalanus vanus	0.11	0.00	0.00
Eucalanidae	*Subeucalanus crassus*	0.53	0.08	0.08
	Subeucalanus longiceps	0.00	0.00	0.13
	Subeucalanus pileatus	1.24	0.38	0.34
	Subeucalanus subcrassus	0.27	0.15	0.07
	Subeucalanus subtenuis	0.00	0.09	0.00
	Subeucalanus copepodid	1.14	1.08	0.00
Euchaetidae	*Euchaeta cocinna*	0.05	0.00	0.00
	Euchaeta indica	0.00	0.00	0.08
	Euchaeta rimana	0.09	0.15	0.00
	Euchaetidae copepodid	2.36	0.09	0.66
Heterorhabdidae	*Heterohabdus papilliger*	0.00	0.00	0.06
Lucicutiidae	*Lucicutia flavicornis*	0.10	0.00	0.00
	Lucicutia gausiae	0.04	0.00	0.00
	Lucicutia ovalis	0.00	0.00	0.06
Mecynoceridae	*Mecynocera clausi*	0.14	0.08	0.08
Metridicidae	*Pleuromamma borealis*	0.04	0.00	0.00
	Metridia copepodid	0.00	0.00	0.22
Paracalanidae	***Acrocalanus gibber***	2.93	6.44	4.36
	Acrocalanus gracilis	0.56	1.57	0.42
	Acrocalanus monachus	0.00	0.50	0.00
	Calocalanus contractus	0.00	0.26	0.07
	Calocalanus gracilis	0.05	0.09	0.33
	Calocalanus monospinus	0.00	0.00	0.13
	Calocalanus pavo	0.00	0.00	0.14
	Calocalanus pavoninus	0.04	1.30	1.10
	Calocalanus plumulosus	0.00	0.66	0.13
	Calocalanus styliremis	0.04	0.82	0.79
	Paracalanus aculeatus	0.20	0.48	1.62
	Paracalanus pavus	15.19	8.22	12.72
	Paracalanus serrulus	3.41	3.10	1.83
	Parvocalanus crassirostris	8.37	21.73	11.04
Pontellidae	*Calanopia elliptica*	0.00	0.08	0.34
	Calanopia minor	0.09	0.18	0.13
	Lobidocera copepodid	0.00	0.00	0.59
	Pontellopsis tenuicauda	0.00	0.08	0.00
Scolecithricidae	*Scolecithricella longispinosa*	1.40	0.00	0.08
	Scolecithrix danae	0.00	0.09	0.00
Temoridae	*Temora discaudata*	0.13	0.08	0.06
	Temora stylifera	0.04	0.24	0.06
	Temora turbinata	4.71	6.71	7.71
	Temoropia mayumbaensis	0.05	0.00	0.00
Tortanidae	*Tortanus forcipatus*	0.05	0.00	0.00

Table 2. (Cont.)

| Family | Species | Assemblage categories | | |
		West Strait	East Strait	East China Sea
Order: Cyclopoida				
Oithonidae	*Oithona atlantica*	0.09	0.08	0.00
	Oithona attenuata	2.03	4.92	3.76
	Oithona brevicornis	3.22	0.46	0.55
	Oithona decipiens	0.16	0.00	0.00
	Oithona fragilis	0.28	0.00	0.00
	Oithona longispina	0.32	0.07	0.00
	Oithona similis	2.12	0.09	0.06
	Oithona simplex	0.10	0.35	0.00
	Oithona plumifera	2.52	1.45	3.76
	Oithona fallax	0.59	0.30	1.37
	Oithona rigida	0.35	0.47	0.35
	Paroithona sp.	0.00	0.08	0.13
Order: Harpacticoida				
Clytemnstridae	*Clytemnestra scutellata*	0.40	0.08	0.00
Ectinosomatidae	*Microsetella norvegica*	0.00	0.00	0.06
	Microsetella rosea	0.46	0.08	0.25
Euterpinidae	***Euterpina acutifrons***	10.39	2.12	0.20
Miraciidae	*Macrosetella gracilis*	0.00	0.08	0.21
Order: Mormonilloida				
Mormonillidae	*Mormonilla minor*	0.00	0.00	0.14
Order: Poecilostomatoida				
Corycaeidae	*Corycaeus flaccus*	0.00	0.00	0.07
	Corycaeus typicus	0.00	0.00	0.07
	Corycaeus speciosus	0.00	0.00	0.13
	Corycaeus affinis	0.36	0.08	0.00
	Corycaeus andrewsi	0.14	0.43	0.25
	Corycaeus asiaticus	0.00	0.00	0.06
	Corycaeus dahli	2.79	3.83	0.41
	Corycaeus erythraeus	0.00	0.00	0.14
	Corycaeus lubbocki	4.94	0.00	0.35
	Corycaeus subtilis	0.66	0.23	0.82
	Corycaeus agilis	0.04	0.09	0.27
	Corycaeus catus	0.04	0.45	1.00
	Corycaeus giesbrechi	0.66	0.55	1.89
	Corycaeus pacificus	0.13	0.34	0.13
	Corycaeus lautus	0.05	0.00	0.00
	Corycaeus longistylis	0.04	0.09	0.00
	Corycaeus pumilus	0.00	0.14	0.00
	Farranula concinna	0.00	0.09	0.00
	Farranula gibbula	0.09	0.83	1.07
	Farranula rostrata	0.00	0.00	0.13
Oncaeidae	***Oncaea conifera***	2.52	2.59	6.31
	Oncaea mediterranea	0.08	0.00	0.41
	Oncaea minuta	0.08	0.09	0.39
	Oncaea similis	0.04	0.16	0.13
	Oncaea venusta	9.09	10.34	11.98
	Oncaea sp.	0.00	0.08	0.00
Sapphirinidae	*Copila mirabilis*	0.00	0.09	0.00
	Corina granulose	0.00	0.00	0.06
	Sapphirina iris	0.00	0.00	0.08
	Sapphirina stellata	0.14	0.00	0.00

water from stations 1-3 as the end-member water of the East China Sea, and stations 8-10 as the end-member water of the western Strait. The remaining stations of 4-7 and 12-15 were conditionally modified from the 2 end-members showing various joining topographies in our cluster analysis, because they are influenced either by the southwestern monsoon or the western Pacific tides. This is evidenced by the southern monsoon which drives the South China Sea water northward during summer (Jan et al. 1995), and the Pacific tides which agitate the Strait water back and forth diurnally (Fig. 2). Accordingly, the oceanic species of southern East China Sea (stations 1-3) were transported to the eastern Strait (Fig. 2), mixed with the local neritic species and thus formed an intermediate assemblage in the eastern Strait (stations 4-6 and 14-15). On the west side, due to huge vo-

Table 3. Relative abundance (%) of fish larvae collected from the northern Taiwan Strait and southern East China Sea. Assemblages are categorized according to hydrographic regions. Dominant species of each region are marked in boldface

Family	Species	Assemblage categories		
		West Strait	East Strait	East China Sea
Order: Calanoida				
Acanthuridae	*Ctenochaetus binotatus*	0.00	0.00	0.68
Ambassidae	*Ambassis* sp.	0.00	0.00	0.46
Ammodytidae	*Embolichthys mitsukurii*	0.78	0.33	0.93
Apogonidae	***Apogon endekataenia***	5.22	0.00	0.93
	Apogon lineatus	0.55	0.00	0.27
	Apogon pseudotaeniatus	0.00	0.45	0.27
Blenniddae	*Omobranchus elegans*	0.00	0.33	0.00
Bothidae	*Engyprosopon multisquama*	1.64	0.00	2.53
	Laeops kitaharae	0.29	0.00	0.00
	Psettina gigantea	1.69	0.00	1.60
Bregmacerotidae	*Bregmaceros arabicus*	0.00	1.82	4.32
	Bregmaceros nectabanus	1.07	0.00	0.00
Callionymidae	*Callionymus beniteguri*	0.00	0.00	1.08
Carangidae	*Caranx sexfasciatus*	0.60	0.00	0.54
	Caranx sp.	0.00	0.00	0.46
	Decapterus macrosoma	0.00	1.82	1.87
	Scomberoides lysan	0.00	0.00	1.19
	Selar crumenophthalmus	1.33	0.00	3.05
Chaetodontidae	Chaetodontid	0.00	0.00	0.27
Champsodontidae	*Champsodon snyderi*	0.00	0.00	1.75
Clupeidae	*Etrumeus teres*	0.60	2.30	0.46
Coryphaenidae	*Coryphaena hippurus*	0.00	0.00	0.27
Creediidae	*Limnichthys fasciatus*	0.00	0.45	0.00
Cynoglossidae	*Cynoglossus joyneri*	1.10	0.00	0.68
	Cynoglossus sp.	0.00	0.45	0.00
	Paraplagusia japonica	0.26	0.00	0.00
	Symphurus orientalis	1.69	2.50	0.00
Emmelichthyidae	*Erythrocles schlegelii*	0.00	0.00	0.81
Engraulidae	***Encrasicholina heteroloba***	7.51	12.00	2.78
	Setipinna tenuifilis	1.58	0.00	0.00
Gerreidae	*Gerres oyena*	0.00	0.99	0.00
Gobbidae	*Amblychaeturichthys hexanema*	0.00	0.33	0.00
	Bathygobius cotticeps	0.78	0.00	0.00
	Parachaeturichthys polynema	0.00	0.33	0.00
Gonostomatidae	*Cyclothone atraria*	0.00	0.33	0.00
	Gonostoma atlanticum	0.49	0.00	0.00
	Maurolicus muelleri	0.00	0.00	0.27

Table 3. (Cont.)

Family	Species	Assemblage categories		
		West Strait	East Strait	East China Sea
Haemulidae	*Hapalogenys nitens*	0.00	0.00	0.68
Labridae	*Xyrichthys* sp.	0.55	0.00	0.93
Leiognathidae	***Leiognathus rivulatus***	5.26	2.76	0.00
	Secutor insidiator	1.71	2.78	2.78
Lethrinidae	*Lethrinus nematacanthus*	0.00	0.00	0.93
Lutjanidae	*Lutjanus bohar*	0.00	0.00	3.26
Monacanthidae	*Rudarius ercodes*	0.60	0.00	0.46
Mugillidae	*Liza affinis*	0.00	0.33	0.00
Mugiloididae	*Parapercis pulchella*	0.00	0.00	0.27
Mullidae	*Upeneus bensasi*	0.00	1.82	1.39
Myctophidae	*Benthosema fibulatum*	0.00	0.00	0.93
	Benthosema pterotum	2.04	0.00	0.93
	Bolinichthys pyrsobolus	0.00	1.91	0.00
	Ceratoscopelus warmingi	0.00	5.78	0.00
	Diaphus pacificus	0.00	1.25	5.20
	Diaphus sp.	0.00	0.45	0.00
	Diaphus theta	0.60	5.00	0.73
	Lampadena luminosa	0.00	1.25	0.00
	Myctophum asperum	0.00	0.00	0.27
Nemipteridae	*Scolopsis* sp.	2.84	0.00	0.00
Ophidiidae	*Sirembo imberbis*	0.00	0.00	0.27
Percichthyidae	*Acropoma japonicum*	0.00	0.00	0.93
	Synagrops philippinensis	0.00	0.00	3.01
Percophidae	Percophid	0.00	0.00	5.86
Pomacentridae	*Chromis* sp.	0.00	0.00	0.93
Priacanthidae	***Priacanthus macracanthus***	0.00	0.33	12.54
Scaridae	*Scarus* sp.	0.00	0.33	1.66
Scatophagidae	*Scatophagus argus*	0.57	1.11	0.68
Sciaenidae	*Argyrosomus argentatus*	1.14	1.36	0.00
	Nibea japonica	0.49	0.00	0.00
	***Nibea* sp.**	17.90	0.00	1.35
	***Pseudosciaena* sp.**	6.62	0.00	0.00
Scombridae	***Auxis rochei***	0.00	4.50	5.44
	Auxis thazard	0.00	2.61	0.93
	Euthynnus affinis	0.00	1.36	0.00
	Euthynnus pelamis	0.00	0.66	0.46
Scorpaenidae	Scorpaenid	0.00	0.99	0.00
Serranidae	*Epinephelus akaara*	0.00	0.00	0.27
	Sacura margaritacea	0.00	0.00	0.93
Sillaginidae	*Sillago japonica*	2.04	0.78	0.93
	Sillago sihama	0.00	0.91	0.00
Soleidae	*Aseraggodes kobensis*	0.29	0.00	0.00
Synodontidae	***Saurida elongata***	9.26	0.00	0.00
	Saurida wanieso	0.55	0.00	0.00
	Synodus macrops	0.00	0.00	0.27
	Trachinocephalus myops	0.00	2.43	0.73
Teraponidae	*Rhyncopelates oxyrhynchus*	0.00	0.00	0.46
Trichiuridae	*Benthodesmus elongatus*	0.00	0.00	0.46
	Trichiurus lepturus	10.62	25.30	7.13
Uranoscopidae	*Gnathagnus elongatus*	0.55	0.00	0.00
	Uranoscopus japonicus	0.00	0.00	0.93
Others		9.18	9.57	7.67

lumes of river runoff (Zhu et al. 1988) and subsurface water upwelling to the surface (Jan et al. 1995), both coastal and neritic species occur in the assemblage of the western Strait (stations 7 and 11-13). Topologies of dendrograms derived from copepods and fish larvae matched fairly well to the hydrographic regions (Figs. 4, 5). In the dendrogram of copepods, cluster A2, consisting of stations 5 and 15, was located in the Tanshui River plume and was thus grouped together with the highest similarity (Figs. 1 and 5). Stations 7 and 13 of cluster A3 were expected to join the cluster of the western Strait (A1), but were grouped into clusters A4 because of their location near the hydrographic boundary (Fig. 1). In the dendrogram of fish larvae, cluster B2 of stations 12 and 13 should be included in the western Strait according to the hydrographic categorization. As they were also located at the hydrographic boundary with complicated flood-ebb tides (Fig. 2), stations 12 and 13

depicted the highest similarity due to the relative scarcity of fish larvae (Fig. 7b), which was unexpected to those of the other stations.

Among dominant species of copepods, *Clausocalanus forcatus*, *Oithona plumifera*, and *Oncaea conifera* (group C, Fig. 6a) were abundant in the East China Sea region (represented by stations 1-3) corresponding to the water mass located
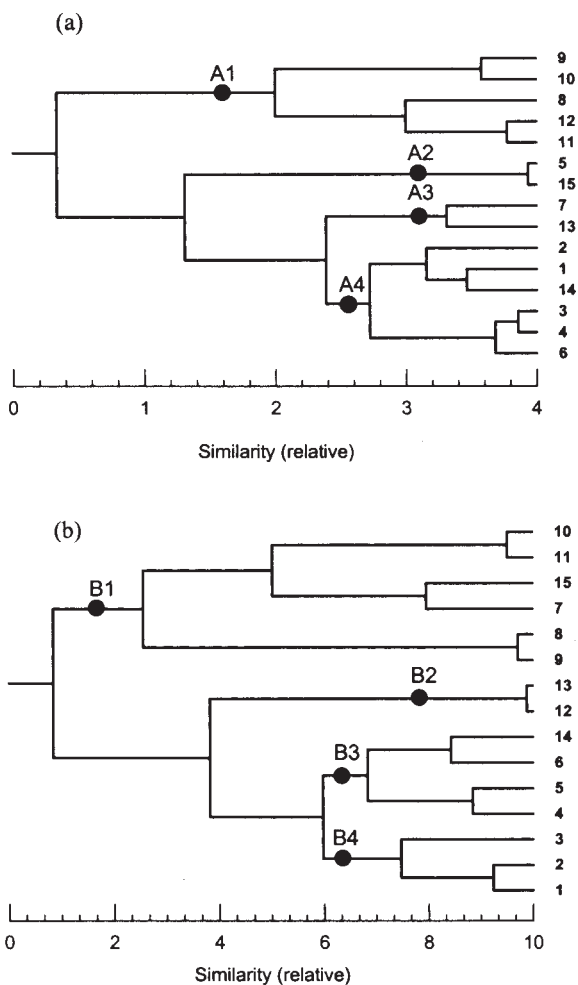
(a)

(b)

Fig. 5. Dendrograms of station association derived from the species composition of copepods (a) and fish larvae (b).
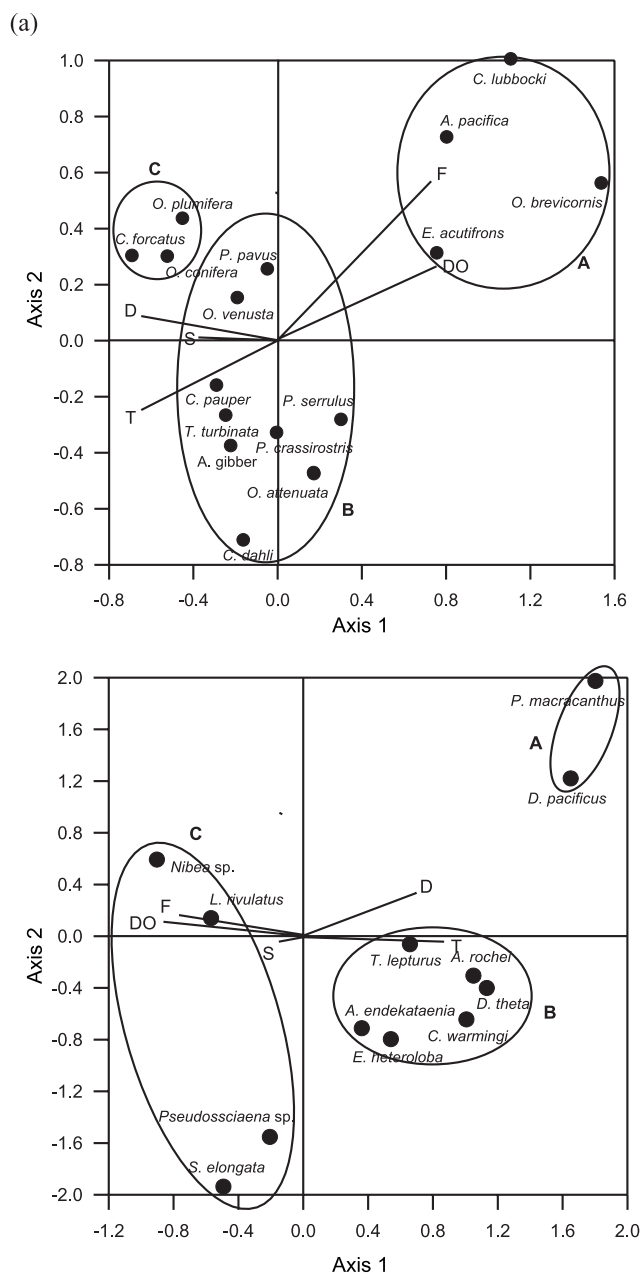
(a)

Fig. 6. Canonical correspondence ordination biplot of dominant species of copepods and fish larvae in relation to hydrographic variables. (D, bottom depth; T, surface water temperature; S, surface water salinity; F, surface water fluorescence; DO, surface water dissolved oxygen; the 3 circles represent the 3 groups of species associations).

where it is deeper, and characterized by high temperature and salinity with low fluorescence and dissolved oxygen at the surface. Four species, *Acartia pacifica*, *Corycaeus lubbocki*, *Euterpina acutifrons*, and *Oithona brevicornis* (group A, Fig. 6a), were confined to shallower water of the Chinese coastal region in the western Strait. The region is characterized by relatively low temperature and salinity but high fluorescence and dissolved oxygen. Ten species, *Acrocalanus gibber*, *Canthocalanus pauper*, *Corycaeus dahli*, *Oithona attenuata*, *Oithona plumifera*, *Oncaea venusta*, *Paracalanus pavus*, *Paracalanus serrulus*, *Parvocalanus crassirostris*, and *Temora turbinate* (group B, Fig. 6a), were relatively widely distributed in the study area so that their distribution pattern was not as pure as the species groups of the end-member waters mentioned previously. According to Chen et al. (1965), Chen and Zhang (1974), and Noda et al. (1998), *Acartia pacifica*, *Corycaeus lubbockii*, *Corycaeus dahli*, *Euterpina acutifrons*, *Oithona brevicornis*, *Paracalanus pavus*, *Paracalanus serrulus*, and *Parvocalanus crassirostris* are neritic species; while *Acrocalanus gibber*, *Canthocalanus pauper*, *Clausocalanus furcatus*, *Oncaea conifera*, *Oncaea venusta*, *Oithona plumifera*, and *Temora turbinata* are oceanic species. With apparently higher tolerance to salinity and temperature fluctuations, *Acrocalanus gibber*, *Canthocalanus pauper*, *Corycaeus dahli*, *Oithona attenuata*, *Oithona plumifera*, *Oncaea venusta*, *Paracalanus pavus*, *Paracalanus serrulus*, *Parvocalanus crassirostris*, and *Temora turbinata* occurred all over the northern Taiwan Strait. In particular, no oceanic species of Chen and Zhang (1974) and Noda et al. (1998) occurred in the Chinese coastal region, but some neritic species (*Acartia pacifica*, *Corycaeus lubbocki*, *Euterpina acutifrons,* and *Oithona brevicornis*) invaded the Chinese coastal region. It is therefore reasonable to propose that the southwestern monsoon brings neritic copepod species to the China coastal region, while the tidal movement brings oceanic copepod species from the East China Sea to the eastern Strait. In fish larva samples, *Diaphus pacificus* and *Priacanthus macracanthus* (group A, Fig. 6b) were abundant in the deeper water of the East China Sea region, characterized by high temperature but low fluorescence and dissolved oxygen. The species of *Leiognathus rivulatus*, *Nibea* sp., *Pseudosciaena* sp., and *Saurida elongata* (group C, Fig. 6b) were abundant in the shallow water of the western Strait, characterized by low surface temperature but high fluorescence and dissolved oxygen. There are 6 species

grouped in correspondence to the medians of measured variables (group B, Fig. 6b), among which *Auxis rochei*, *Diaphus theta*, and *Ceratoscopelus warmingy* were abundant in the eastern Strait; *Apogon endekataenia* in both the western Strait and East China Sea; and *Encrasicholina heteroloba* and *Trichiurus lepturus* were widely distributed throughout the study area. The dominant fish larvae found in the East China Sea are consistent with those reported by Huang and Chiu (1998). Larvae of *Encrasicholina heteroloba* were found abundantly in both the eastern Strait and East China Sea, and are an important commercial species from May to September (Huang and Chiu 1998). The fish faunas in the northern Taiwan Strait are distinct in the 3 regions due to hydrographic variations.

The oceanographic data show that river runoff from mainland China and upwelling water along the Chinese coast bring nutrients into the western
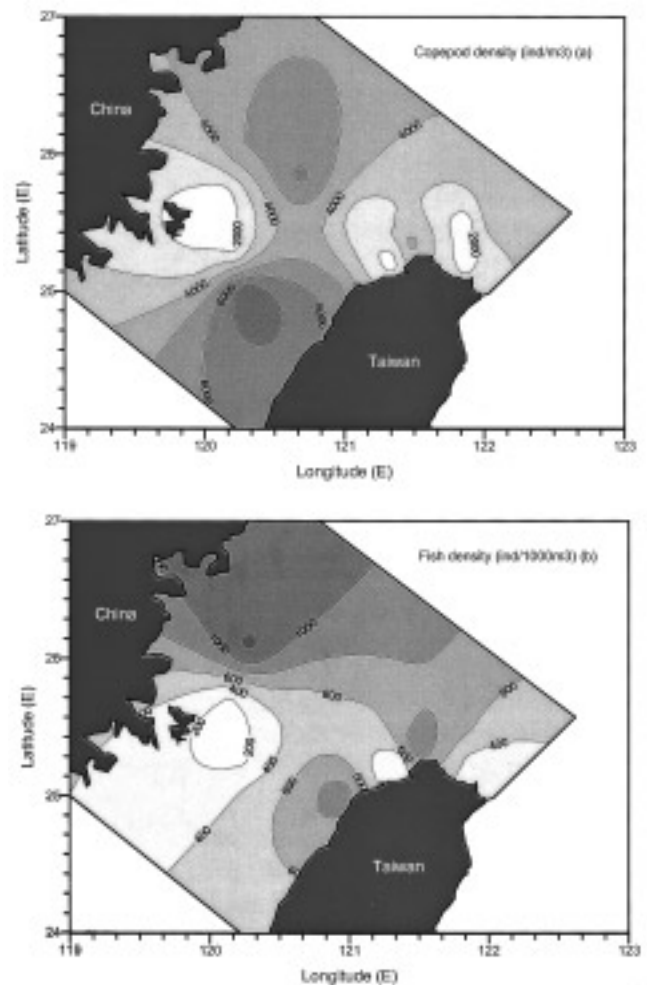

Fig. 7. Contour plots of copepod abundance (a) and fish larvae abundance (b) in waters of the northern Taiwan Strait.

Strait region. In this study, the input of nutrients resulted in a phytoplankton bloom as represented by fluorescence indices (Fig. 3c). Copepod abundance was negatively related to fluorescence. Areas of peak copepod abundance did not correspond to areas of high primary production but were in the marginal zone outside the high production area (Fig. 7a). It has been shown that phytoplankton develop over time on stable sides of a front or mixing area, which provides a more suitable place for zooplankton (Lalli and Parsons 1993, Maravelias and Reid 1997). This is supported by our study, which reveals an up- and down-stream relationship between primary production and copepod abundance. Other factors appearing to have effects on copepod abundance as shown in this study were temperature and dissolved oxygen. Our results support those studies showing that copepod production is temperature dependent (Huntley and Lopez 1992 and references therein) and that copepod distribution is constrained by dissolved oxygen (Roman et al. 1993).

This work has extended our knowledge of fish larvae and copepods in the northern Taiwan Strait. In our study, *Trichiurus lepturus* and *Encrasicholina heteroloba* were dominant larval fish species, and *Paracalanus pavus*, *Parvocalanus crossirostris*, *Oncaea venusta*, and *Temora turbinata* were dominant copepod species in the northern Strait in summer with high abundance and wide distribution. *Trichiurus lepturus* and *Encrasicholina heteroloba* are also important fishery resources in this area. We tried to relate the abundance of the 2 dominant species of fish larvae with the 4 dominant copepod species, but the outcome from correlation analysis implied that the relationship was weak. Gut content analysis of the larvae of the Japanese anchovy *Engraulis japonicus* revealed that their diet composition primarily consisted of copepodites of *Paracalanus* and *Oithona* species (Hirakawa and Ogawa 1996, Hirakawa et al. 1997). The abundance of *Paracalanus* and *Oithona* species was very high in our study area. Further studies on gut content analysis and more intensive sampling are necessary to address the trophic relationships among dominant species of fish larvae and copepods. Incorporation of biological/physical modeling synthesis is also needed for better understanding of the hydrographic effects on trophoecology in the Taiwan Strait.

REFERENCES

Boucher M. 1984. Localization of zooplankton populations in the Ligurian marine front: role of ontogenetic migration. Deep-Sea Res. **29:** 953-965.

Boucher M, F Ibanez, L Prieur. 1987. Daily and seasonal variations in the spatial distribution of zooplankton populations in relation to the physical structure in the Ligurian sea front. J. Mar. Res. **45:** 133-173.

Braak CJF. 1994. Canonical community ordination. Part I: Basic theory and linear method. Ecoscience **1:** 127-140.

Chen QC. 1992. Zooplankton of China Seas (1). Beijing: Science Press.

Chen QC, SZ Zhang. 1974. The planktonic copepods of the Yellow Sea and the East China Sea. 1. Calanoida. Stud. Mar. Sinica **7:** 20-133. (in Chinese)

Chen QC, SZ Zhang, CS Zhu. 1965. On planktonic copepods of the Yellow Sea and the East China Sea. 2. Cyclopoida and Harpacticoida. Stud. Mar. Sinica **9:** 27-100. (in Chinese)

Chiu TS, KZ Chang. 1994. Comparison of ichthyoplankton fauna in northern Taiwan Strait during winter and spring. Acta Zool. Taiwanica **5:** 23-31.

Chiu TS, KZ Chang. 1995. Diurnal cycling in vertical distribution of ichthyoplankton at a fixed station off northwestern Taiwan. Zool. Stud. **34:** 183-192.

Fang KL. 1982. A study of water masses in Taiwan Strait. Acta Oceanogr. Taiwanica **13:** 140-153.

Fang KL, CY Yu. 1981. A study of water masses in the seas of southernmost Taiwan. Acta Oceanogr. Taiwanica **12:** 94-111.

Fernandez E, J Cabal, JL Acuna, A Bode, A Botas, C Garcia-Soto. 1993. Plankton distribution across a slope current-induced front in the southern Bay of Biscay. J. Plankton Res. **15:** 619-641.

Gauch HG. 1983. Multivariate analysis in community ecology. New York: Cambridge Univ. Press.

Hirakawa K, T Goto, M Hirai. 1997. Diet composition and prey size of larval anchovy, *Engraulis japonicus*, in Toyama Bay, southern Japan Sea. Bull. Jpn. Natl. Fish. Res. Inst. **47:** 67-78.

Hirakawa K, Y Ogawa. 1996. Characteristics of the copepod assemblage in the southwestern Japan Sea and its implication for anchovy population dynamics. Bull. Jpn. Natl. Fish. Res. Inst. **46:** 45-64.

Hsieh CH, TS Chiu. 1998. Copepod abundance and species composition of Tanshui River estuary and adjacent waters. Acta Zool. Taiwanica **9:** 1-9.

Huang JB, TS Chiu. 1998. Seasonal and hydrographic variations of ichthyoplankton density and composition in the Kuroshio edge exchange area off northeastern Taiwan. Zool. Stud. **37:** 63-73.

Huntley MK, MDG Lopez. 1992. Temperature-dependent production of marine copepods: a global synthesis. Am. Nat. **140:** 201-242.

Jan S, CS Chern, J Wang. 1994. Influences of sea surface wind stress on summertime flow pattern in the Taiwan Strait. Acta Oceanogr. Taiwanica **33:** 63-80. (in Chinese with English abstract)

Jan S, CS Chern, J Wang. 1995. A numerical study on currents in Taiwan Strait during summer time. La Mer **33:** 23-40.

Krebs CJ. 1989. Ecological methodology. New York: Harper & Row.

Lalli CM, TR Parson. 1993. Biological oceanography: an introduction. Oxford: Pergamon Press.

Maravelias CD, DG Reid. 1997. Identifying the effect of oceanographic features and zooplankton on prespawning herring abundance using generalized additive models. Mar. Ecol. Prog. Ser. **147:** 1-9.

McCulliagh P, JA Nelder. 1983. Generalized linear model. New York: Chapman & Hall.

Noda M, I Ikeda, S Ueno, H Hashimoto, K Gushima. 1998. Enrichment of coastal zooplankton communities by drifting zooplankton patches from Kuroshio front. Mar. Ecol. Prog. Ser. **170:** 55-65.

Pielou EC. 1984. The interpretation of ecological data. New York: Wiley.

Poulet SA, R Williams. 1991. Characteristics and properties of copepods affecting the recruitment of fish larvae. Bull. Plankton Soc. Jpn. Spec. pp. 271-290.

Roman, MR, AL Gauzens, WK Rhinehart, JR White. 1993. Effects of low oxygen waters on Chesapeake Bay zooplankton. Limnol. Oceanogr. **38:** 1603-1614.

Tan TH. 1967. On the distribution of copepods in waters surrounding Taiwan. Rep. Inst. Fisher. Biol., Ministry of Economic Affairs and National Taiwan Univ. **2:** 14-20.

Thomas AC, WJ Emery. 1986. Winter hydrography and plankton distribution on the southern British Columbia continental shelf. Can. J. Fish. Aquat. Sci. **43:** 1249-1258.

Tremblay MJ, JC Roff. 1983. Community gradients in the Scotia shelf zooplankton. Can. J. Fish. Aquat. Sci. **40:** 598-611.

Tzeng WN, YT Wang. 1992. Structure, composition and seasonal dynamics of the larval and juvenile fish community in the mangrove estuary of Tanshui River, Taiwan. Mar. Biol. **113:** 481-490.

Tzeng WN, YT Wang. 1993. Hydrography and distribution dynamics of larval and juvenile fishes in the coastal waters of the Tanshui River estuary, Taiwan, with reference to estuarine larval transport. Mar. Biol. **116:** 205-217.

Xiao H. 1988. Studies of coastal upwelling in western Taiwan Strait. J. Oceanogr. Taiwan Strait **7:** 135-142. (in Chinese with English abstract)

Zheng Z, SJ Li, S. Li, BY Chen. 1982. On the distribution of planktonic copepods in Taiwan strait. Taiwan Strait **1:** 69-79. (in Chinese with English abstract)

Zhu CS, JZ Wu, YS Lin, M Su, CJ Huang, QB Hu. 1988. The species composition, distribution and abundance of plankton. *In* Fujian Institute of Oceanography, ed. A comprehensive oceanographic survey of the central and northern part of Taiwan Strait. Beijing: Science Press, pp. 259-305. (in Chinese)

臺灣海峽北部橈腳類及仔魚對應於夏季水文之分布

謝志豪　丘臺生

　　本研究之目的在於分析橈腳類及仔魚對應於臺灣海峽中尺度之水文狀態之分布情形。研究時間為夏季西南季風盛行時。海流資料顯示，漲潮時東海水流入海峽東側，退潮時海峽水退至東海南部。依據表水之溫度及鹽度等值分布圖以及水團之鹽溫線圖分析，此時海峽可依中線區隔為二，東側為南海表水及東海水之混合區，而西側則表現出南海次表層水在近海區湧升之現象。此研究在海峽及北臺灣水域探測之測站可區分為三個水文區：即東海峽區、西海峽區及東海區。西海峽之表水具相對之低溫高鹽，證為源於澎湖水道之南海水所湧升。東海峽表水具高溫低鹽，然而東海水則為高溫及次高鹽之狀態(稍低於西海峽水)。以聚類分析法針對橈腳類及仔魚群集進行分析，結果各顯示四個叢集，其中有三個叢集所定義的群集分別對應於三個水文區，即東海峽群、西海峽群及東海群；後兩者為主要群。西海峽群由沿岸及近海物種所組成，東海群主要為外洋物種，東海峽群在兩主要群之中間地帶屬混合群，有近海及外洋物種。典型對應分析顯示，橈腳類及仔魚群集組成之變異可由海峽北部之水文因子所解釋。由迴歸分析顯示，橈腳類之密度與水溫及溶氧量呈正相關，但密度最高之橈腳類出現區並不與最高之初級生產區域相吻合，卻出現在湧升流區外圍之穩定海區。仔魚密度與橈腳類之密度分布則呈統計上之一致性。

關鍵詞：物種組成，西南季風，南海，東海，湧升流。

國立臺灣大學動物學系